Open Access

Novel Electromagnetic-Interference-Free Indoor Environment Monitoring System by Mobile Camera-Image-Sensor-Based VLC
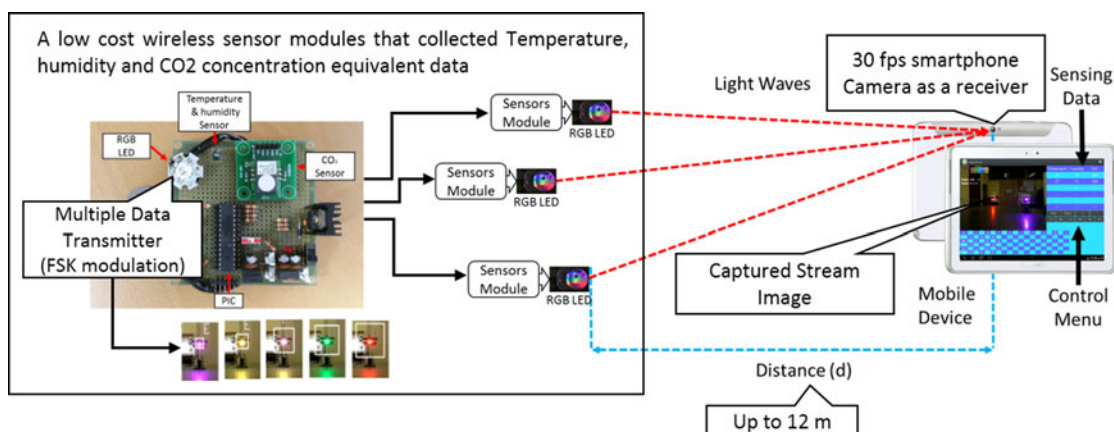
ZhenYang Ong
Vega Pradana Rachim
Wan-Young Chung, *Member, IEEE*

Novel Electromagnetic-Interference-Free Indoor Environment Monitoring System by Mobile Camera-Image-Sensor-Based VLC

**ZhenYang Ong, Vega Pradana Rachim,
and Wan-Young Chung, *Member, IEEE***

Department of Electronic Engineering, Pukyong National University,
Busan 608-737, South Korea

Abstract: Long-term exposure to radio frequency waves can have adverse effects on hu-
man health. It may cause bad effects especially to elderly people, children, and patients
with weak immune systems. On the other hand, visible light communication technologies
that use a light-emitting diode (LED) light source and a photodetector to transmit and re-
ceive data through visible light have a severe demerit that the modulation and demodulation
processes in the system can be complicated. This paper presents a low-cost wireless mo-
bile indoor environment monitoring system with no additional complicated signal detecting
device, except a mobile device and sensor modules. Temperature, humidity, and CO_2 con-
centration equivalent data are collected by sensor modules, and these data are modulated
using frequency shift keying modulation. The modulated data are transmitted wirelessly by
using a red–green–blue LED for transmitting multiple data concurrently. An Android applica-
tion is developed to act as a light-signal receiver from multiple sensor modules. The image
stream of the LED is captured and is processed locally in a mobile device. A single-receiver
module with a camera image sensor can accept sensing data from six sensor modules
simultaneously with a maximum transmission range up to 12 m and low error rate.

Index Terms: Indoor environment monitoring, temperature sensor, humidity sensor, CO_2
sensor, camera image sensor, visible light communication.

1. Introduction

In recent years, the demand for monitoring systems for various purposes in different fields has
increased dramatically. To increase the efficiency of the workforce, wireless monitoring systems
are implemented for achieving better monitoring performance with low cost, high reliability, and
convenience [1]. Among the wireless monitoring systems, the indoor-environment monitoring sys-
tem is one of the systems in high demand [2]–[4]. Indoor-environment (such as house, hospital,
or office) monitoring is needed to guarantee a comfortable and healthy environment for the people
living in it. This monitoring system is very important, especially for elderly people, children, and
patients with weak immune systems. Air temperature, humidity, and CO_2 concentration level are

the three important factors for a satisfactory indoor environment. Most of the researches on indoor environment monitoring systems have used a radio frequency (RF) wireless communication medium or a wired communication technique. However, long-term usage of RF communication for wireless data transmission may deteriorate human health and cause adverse biological effects in the human body. In addition, RF technology generates electromagnetic interference (EMI), which not only jeopardize the performance of the medical instruments in the hospital but also cause malfunction of medical devices implanted in patients [5]–[7]. Unfortunately, these negative facts result in a situation that is the opposite of the original concept behind the indoor environment monitoring, which is to generate a healthy environment. Visible light communication (VLC) technology is one of the wireless communication methods which can act as a substitute for the existing RF communication methods. The EMI-free and hazardless properties of VLC not only make VLC a better long term wireless communication technique for indoor environments but also support the possibility of implementing wireless communication in RF-sensitive areas [8], [9]. Additionally, highly secure and low cost wireless communication can be achieved owing to the line-of-sight (LOS) transmission and utilization of the unlicensed visible light spectrum from 380 nm to 780 nm as the transmission medium in VLC. In normal VLC, the original data are transmitted by fast-switching light-emitting diodes (LEDs) at the modulation module, and the transmitted signal is received using photodetectors (PDs) at the demodulation module. Ultra-high speed PD-based VLC has been developed by the utilization of high response-speed Avalanche photodiodes (APDs) and the implementation of modulation schemes with high spectral efficiencies [10]–[13]. Ultra-high speed multichannel transmission has also been realized through the implementation of multiplexing techniques or multiple-input-multiple-output (MIMO) technology [14]–[16]. However, the short transmission distances in these researches had limited their usability despite the ultra-high speed transmission. Use of lenses or laser diodes is proposed to overcome the data transmission distance limitation [17]. However, only minor improvement is achieved with external lenses, and high-power laser rays may be harmful to humans. Besides, the limited availability of high-speed PDs and the requirement of an external demodulation and signal-processing module have reduced the practicality and efficiency of the low cost application of VLC. Thus, the image sensor (IS) module, which consists of a two-dimensional (2-D) array of PDs, is proposed to be used as the receiver in the VLC system owing to the high availability and enhanced performance of IS compared to PD [18], [19]. High-speed VLC transmission systems for distances less than 50 cm were developed using the complementary metal-oxide semiconductor (CMOS) IS of a camera with the rolling-shutter method [20], [21]. The ability of the IS to spatially separate the signal sources also equips the VLC system with multi-transmission features. Single frame multi-transmission was successfully developed using a display device and a camera system [22], [23]. Although high data rates are achieved in both methods, each has some drawbacks. The rolling shutter method has a limited transmission distance and high data loss rate. In the screen-to-camera-based method, a large size high cost transmitter is needed and high complexity compensation algorithms are required to compensate for the variations in the angle of the camera view. For remote sensing of environment, long range over 10 m and multiple sensing data transmissions are required. In our previous report, the mobile long range VLC was also reported using LEDs and built-in camera of mobile device [24], [25]. This paper introduces a mobile environment monitoring system which utilizes an improved camera sensor-based VLC wireless transmission method in a practical indoor environment. The mobile remote monitoring system receives the sensing data from multiple locations in long range, and real-time transmission is implemented in the mobile monitoring system. Temperature, humidity, and CO_2 concentrations are received from various sensor modules at multiple locations simultaneously by using the camera and analyzed in the mobile device. An alert system can also be equip with the monitoring system which used for warning the user.

2. System Design and Implementation

The proposed mobile camera IS-based VLC environment monitoring system consists of multiple sensor modules with VLC transmitter for data sensing at multiple locations and an Android-based
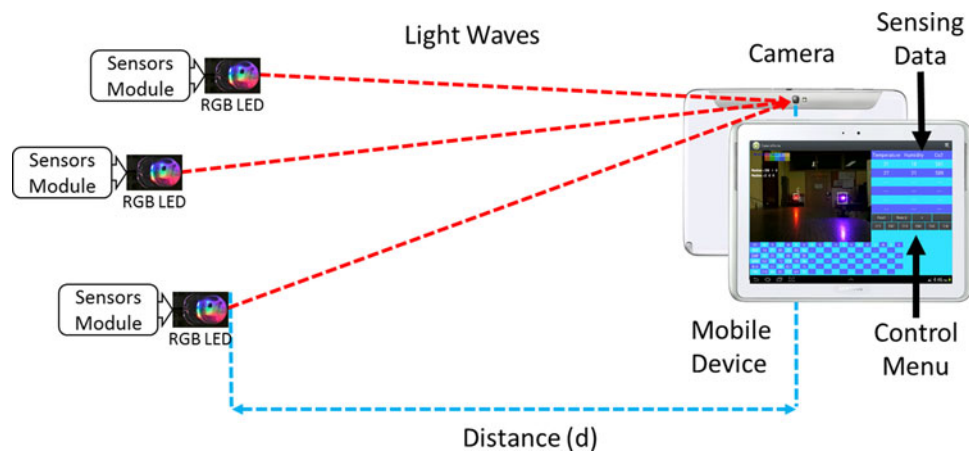
Fig. 1. Proposed system architecture for mobile indoor environment monitoring system using camera sensor-based VLC.

mobile device with a built-in camera. Fig. 1 illustrates the system architecture of the proposed system. Temperature, humidity, and CO_2 concentration are selected as the key parameters to be monitored in indoor for a healthy and comfortable environment for humans. The sensing data are collected from the sensors, processed by the sensor module, and modulated onto light beams. Red-green-blue LED (RGB LED) which comprise of red, green, and blue elements within single housing is used as a light emitter to emit colored light beam. At the same time, the camera IS module of a mobile device is used to capture the signals from the transmitters. An Android application is developed for image processing and data reconstruction in the mobile device. Multiple sensor modules transmit simultaneously from several locations at different line-of-sight distance. As the CMOS IS has the ability to spatially separate the sources, a single receiver (single CMOS IS) is sufficient to receive the sensing data from all transmitters simultaneously. Finally, the received data is displayed on the display of the mobile device.

2.1 A Sensor Module With VLC Transmitter

A sensor module consists of a temperature and humidity sensor (SHT11, Sensirion Inc., USA), an indoor air quality sensor (iAQ-engine, AppliedSensor, Germany), a PIC processing unit, and a 3 Watt RGB LED (Shenzhen Fedy Technology Co., Ltd., China) with LED driver as shown in Fig. 2. Sensors used in the transmitting module have sensing range from 40 °C to 124 °C for temperature, 0 to 100% RH for humidity, and 0 to 2000 ppm for the CO_2 concentration equivalent data. The sensing data are retrieved using the I2C communication protocol, and are further processed in a processing unit. The data is then encapsulated in data packet and modulated using the frequency shift keying (FSK) modulation scheme. An LED driver is used to amplify current supplied to the RGB LED while RGB LED is used to generate multiple number of mixed color lights, rather than three basic colors red, green, and blue. In other words, a balanced mixture of red color light and green color light results in yellow color light while pink color light is obtained from a balanced mixture of red color light with blue color light. The 120 radiation angle of the RGB LED emits widely spread colored light to the front target. A clearer signal can be captured by the camera IS, and the color light intensity does not change much within the camera field of view (FOV).

2.2 A Receiver Module

The camera system and the processing unit of the mobile device are the most important parts in the receiver module which is used for signal acquisition and data processing in a mobile VLC system. A high resolution image with fast frame rate can be captured using a high-end camera
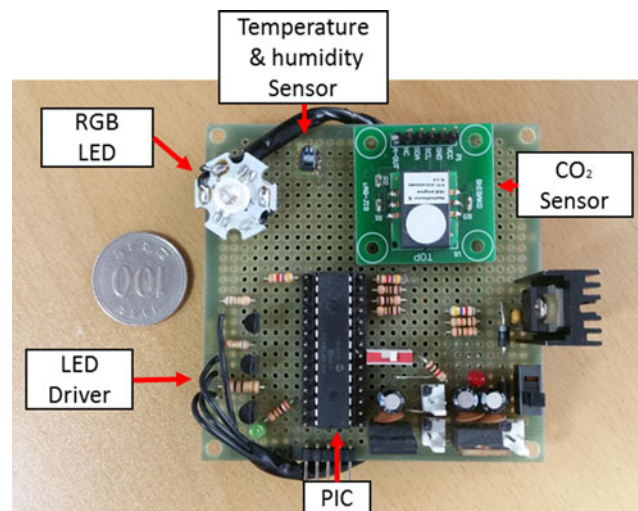
Fig. 2. VLC sensor module with environment sensors and modulation circuit.

while high processing power can be obtained using high-end processing units. Although these factors play important roles in the receiver module, yet the cost of the mobile device is normally proportional to these factors. As the environment monitoring system is developed under conditions of low cost and low complexity wireless transmission, a mid-range tablet PC (Samsung Galaxy Note 10.1, Korea) with a 5-Megapixel CMOS camera and 561 FOV is selected as a receiver without the need of external device to be attached to the receiver. In a mobile camera sensor-based VLC system, the data signal is captured using the camera, and the frame rate of the camera system is equal to the sampling rate of the system. Image size of 768×512 is used rather than using the full resolution of camera because high resolution is not necessary and is redundant. High resolution with more pixels could also slow down the processing speed and frame rate of the camera. The frame rate of the camera in a mobile device is highly dependent on the CMOS sensor exposure time, image readout time, image processing time, and random delay. The frame rate of the camera is inversely proportional to the summation time of these factors. The CMOS sensor exposure time can be set at a constant while the image readout time and the image processing time are consistent. The random delay is the main cause of inconsistency of frame rate and it is caused by the operating system and the background processes that have high priority in the system. According to the Nyquist-Shannon sampling theorem, the sampling rate of the system must be greater than or equal to two times the data rate in order to achieve reliable and accurate data [11]. Thus, due to the limitation of the available smartphone camera frame rates (sampling rate, which is around 30 Hz), we determine our data rate by dividing the sampling rate by 4, with the consideration of data redundancy to reduce the error rate, and to overcome the inconsistency due to the random delay from the Android processing system.

3. Communication Protocol and Software Design for Mobile Monitoring

3.1 Data Packet Structure

The data packet used in the proposed VLC system is composed of 8 bits header, 8 bits temperature data, 8 bits humidity data, 12 bits CO_2 concentration data, 1 bit parity bit and 2 end bits. A parity bit is added for bit error detection which may be caused by blockage of obstacles, data miss, or delay in the system. As asynchronous transmission is implemented in the VLC wireless transmission system, a header byte and two end bits are used for synchronization in the receiver system. A header byte is used as an indicator for the start of the packet, while the end bits are used as
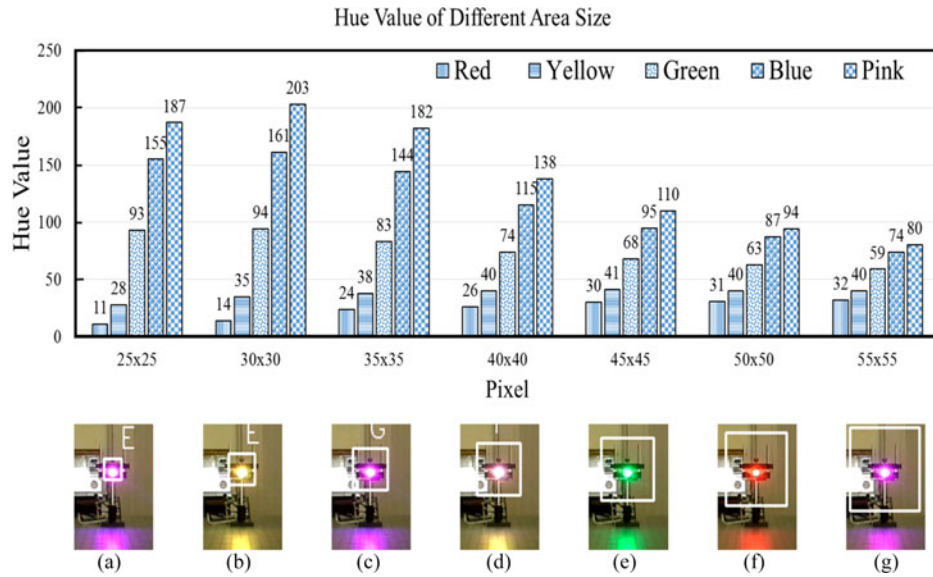
Fig. 3. Hue value variations according to different square areas of R, G, and B lighting.

indicator for the end of each packet. After a header is identified, the following data will be 28 bits payload and 1 parity bit.

3.2 Mobile Camera Sensor-Based VLC

In the proposed mobile camera sensor-based VLC communication system, the data is modulated by the FSK modulation scheme in which the data is modulated onto the carrier frequency by varying the frequency of the carrier frequency. The carrier frequency in the VLC system are represented by light beam, different colors of light beam which have different frequency are used to represent different data. The data are modulated onto the light beam by varying the color of light and transmitted using the RGB LED in the transmitter. In the receiver, the CMOS camera IS is used for signal detection rather than typical PD sensor. Utilization of the CMOS IS in a mobile camera as a PD can increase the transmission distance in the VLC system, and allow multichannel transmission by using a 2-D array of PD within the CMOS IS. The image stream is captured using the CMOS camera and the Hue-Saturation-Value (HSV) of the color light signal is extracted from every image in the image stream. The extracted color information is demodulated back into binary data using a lookup table. The data packet is searched from data string, the sensor data is extracted from the data packet, and the parity bit is checked. The data with correct parity are accepted and displayed while data with error parity will be discarded. In the proposed system, a CMOS camera is used as a receiver for capturing the light signal. However, the background and ambient light from various light sources are also included in the images in addition to the light signal. Hence, the colored light signal must be cropped out from every image. A square shape detection area which bounds the colored light signal is selected manually by the user from the display of the mobile device. The HSV value is extracted from the detection area and the HSV value of the detection area is calculated using

$$HSV_{avg} = \left[\frac{\sum_{i=0}^{n-1}\sum_{j=0}^{m-1} H_{ij}}{n * m}, \frac{\sum_{i=0}^{n-1}\sum_{j=0}^{m-1} S_{ij}}{n * m}, \frac{\sum_{i=0}^{n-1}\sum_{j=0}^{m-1} V_{ij}}{n * m} \right] \tag{1}$$

where n is the width of the detection area and m is the height of the detection area. The size of the colored light signal in the image can be varied with the consideration of the distance between the transmitter and the camera. In Fig. 3, the hue values are extracted from different detection areas at fixed distance of 2m between the LED light source transmitter and the camera IS. Large

differences of hue values between each color are obtained when a proper size is selected. As the size of the detection area increases, the ratio of the signal radiation area to the background increases. A large background area included within the detection area causes the variations in the hue values of the LED image decreased. The large variation in the hue value of the LED image is averaged by the constant hue value of the large background. When the size of the detection area is decreased, partial of signal radiation area is excluded and the variation in the hue value of the LED image decreases. As shown in the result, a detection area of 30 pixel^2 in Fig. 3(b) is the most suitable area for color detection. The hue differences between each color in the 30 pixel^2 detection area are 21, 59, 67, and 42, and are the highest among other size of detection area. However, detection areas with sizes ranging from 25 pixel^2 to 50 pixel^2 are usable, as the differences in the hue values between each color are sufficient for color classification. The 55 pixel^2 detection area is not usable as the differences in the hue values between each color are small and insufficient for accurate classification. The difference between blue and pink is only 7. Small differences between each color may lead to misclassification in the classification algorithm. Misclassification of color by the system may cause data loss or error in data reconstruction.

3.3 Data Rate and Synchronization

As mentioned before, due to the limitation of the frame rate of the camera and the Nyquist-Shannon sampling theorem for the minimum sampling rate, increment of the bit representation of a symbol is proposed in this system to increase the data rate further. In the proposed system, the bit representation of a symbol uses four colors with different frequencies. Red, yellow, green, and blue colors are used for data mapping, with each color carrier frequency are 480 THz, 521 THz, 571 THz, and 645 THz, respectively and each color represents 2 bits of data. One additional color, pink, is the reference signal which is used for signal synchronization in the receiver. After the data packet is constructed in the sensor module, it is split into 20 small packets containing 2 bits each. Then, each packet is modulated to the corresponding color based on the lookup table, and the reference signal is added in front of each packet. RGB LED is used to emit the modulated colored light signals in sequence. During data reconstruction, the reference signal is used as an indicator of the next new data as every new data is led by a reference signal. By utilizing one of the LED in the LED array, the reference signal is emitted as an indicator for selecting an appropriate frame in order to avoid repetition of the data collected caused by inconsistencies of camera frame rate [23]. Although the error is compensated, yet the extra LED not only increases the size of the transmitter but also limits the transmission distance because of perspective distortion of the camera over long distance. Three-channel transmission using a digital single-lens reflex (DSLR) camera and RGB LED is also proposed [26]. Error is minimized by using a DSLR camera with a highly consistent frame rate, and an offline data processing method is implemented. However, the error is not eliminated and is accumulated despite the fact that the error is being suppressed. In the proposed method, the reference signal is implemented by the colored light beam emitted using a single RGB LED. A self-clocking signal is transmitted using a combination of the reference signal and data signal. Hence, time is no longer critical in data reception. The proposed method not only has the same functionality in error compensation, the necessity of data-rate synchronization has also been eliminated with the self-clocking signal.

3.4 ASHREA Standard

A healthy and comfortable environment is the main concern of the indoor-environment monitoring systems in this study. Therefore, three factors temperature, relative humidity, and air quality are selected as the parameters to be monitored. Temperature and humidity are two important factors in the seven major determinants of the thermal comfort of an indoor environment [27]. If the environment temperature is not properly monitored, the human body will be unable to adapt to the environment temperature which might result in heat strokes or freezing to death. High relative humidity in the environment can lead to microbial growth due to the likelihood of condition needed

for the growth of microbial, while low relative humidity can cause skin dryness, irritation of the mucus membranes, and dryness of eyes. Other than the thermal conditions, air quality is the most important factor in human life support. Bad air quality can cause serious adverse effects in humans. Therefore, the level of volatile organic compounds (VOCs) in air is measured, and converted into CO_2 concentration equivalent prediction data which can also be used as an indicator of the indoor environment air quality. Although CO_2 is harmless to humans, it might cause suffocation when its concentration of CO_2 rises to a deleterious level owing to bad ventilation systems or high occupancy within an enclosed space. In this system, the ASHREA Standard 55-2013 [28], Thermal Environmental Conditions for Human Occupancy and ASHREA Standard 62.1-2013 [29], Ventilation for Acceptable Indoor Air Quality are used as references. An indoor environment temperature in the range between 19.4 °C and 27.8 °C is considered comfortable by 80% or more of the test subjects. The environment humidity level recommended is 65% or lower. The CO_2 concentration below 700 ppm in the indoor environment is considered as a good level while the range between 700 ppm and 1000 ppm is considered as acceptable level. CO_2 concentrations above 1000 ppm can cause humans to feel drowsy and CO_2 concentrations above 2500 ppm can caused adverse health effects in humans. The alarm warning system becomes operational if the reading goes out of this range for 1 minute.

4. Experimental Setup

4.1 Environment Monitoring From Multiple Locations in Indoor Area

The proposed environment monitoring system is set up in an office environment within a space of 8.8 m (length) × 7.3 m (width) × 3 m (height) as shown in Fig. 4 for the feasibility test. Two sensor modules with separate VLC transmitters are located at different indoor locations and a mobile device with a CMOS camera is used as the signal receiver in the test system. The RGB LEDs and the camera of the mobile device are in the LOS of each other without any obstacles between them. The LEDs are located within the FOV of the camera of the mobile device. The first LED module with sensors is located at one end of the office at a transmission distance of 7.8 m, 4 to the left of the center of the camera. The second LED module with sensors is located at the center of the office at a transmission distance of 4.2 m, 7 to the right of the center of the camera. All devices are located at a height above 2 m to avoid obstruction cause by humans. The environment sensing data from the sensor module is transmitted to a mobile camera at a data rate of 8 bit/s. The average light intensity in the office environment is 471.6 lux. The user interface for the system is shown in Fig. 4. It consists of four sections a camera view for displaying the captured images, a HSV display section, sensor data display section, and a control panel. The camera view is used to display the captured moving images from the test areas where the RGB LEDs of the sensing modules are located, while the HSV display section shows the HSV value for every color in each channel. As the processing power consumption increases linearly with the number of data transmission channels, in the designed user interface, the maximum number of simultaneous data transmission channels is limited to six (from the six sensing modules) in order to maintain reliable transmission. However, we only tested two channel environment monitoring with the two sensing modules at different locations. Temperature, humidity, and CO_2 concentration equivalent data were shown on the data display section, and the control panel was used for channel selection, data recording, and resetting. A short exposure period was set in order to achieve a high frame rate. Thus, the captured image was underexposed owing to the high frame rate.

5. Results and Discussion

5.1 Indoor Environment Monitoring

Fig. 5 shows the two sets of hue values calculated from two data signals in a single image captured by the camera. The five different hue levels in each set of data are five different demodulated colors from the captured image. Classification is carried out based on the characteristics of the pure color
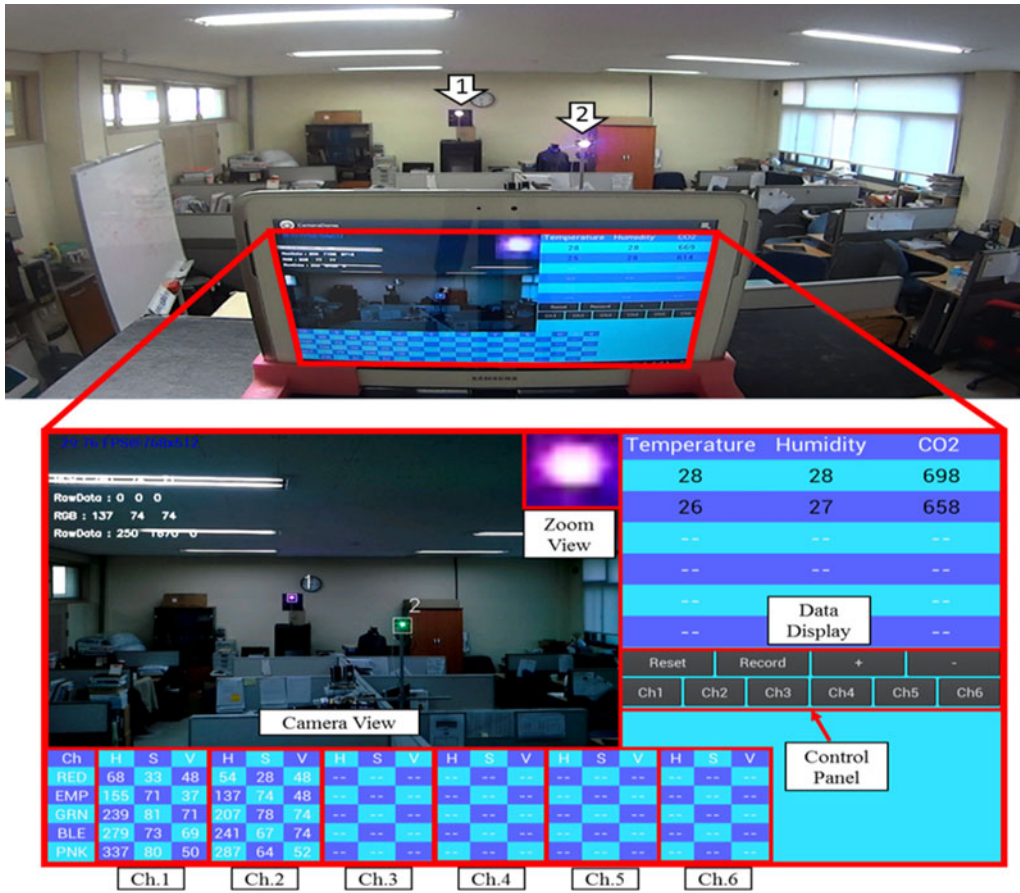
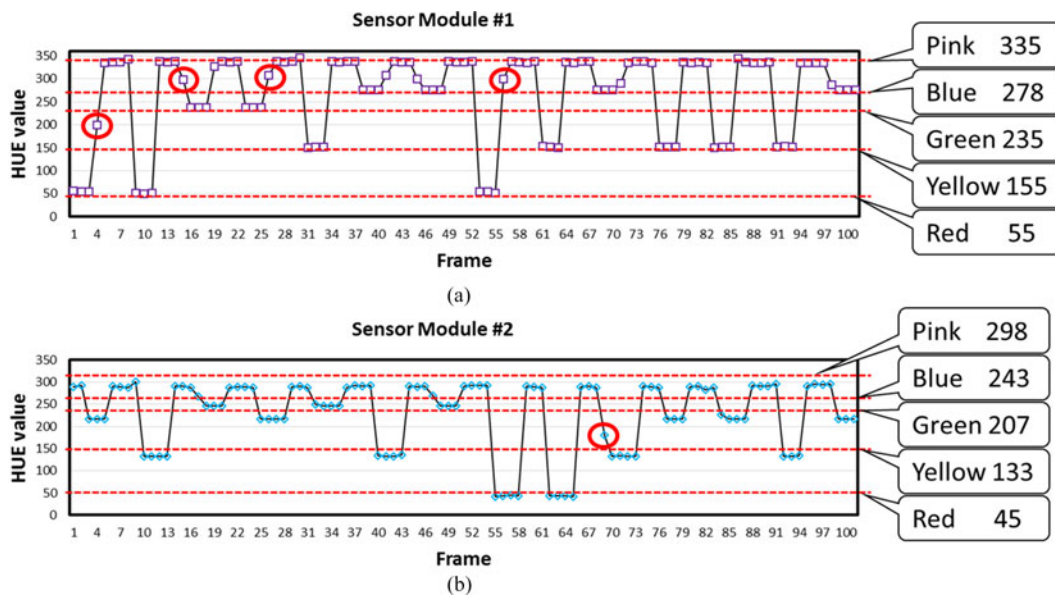Fig. 4. Experimental setup for multilocation monitoring.

Fig. 5. Changes in hue value detected at the receiver. (a) Sensor module #1. (b) Sensor module #2.
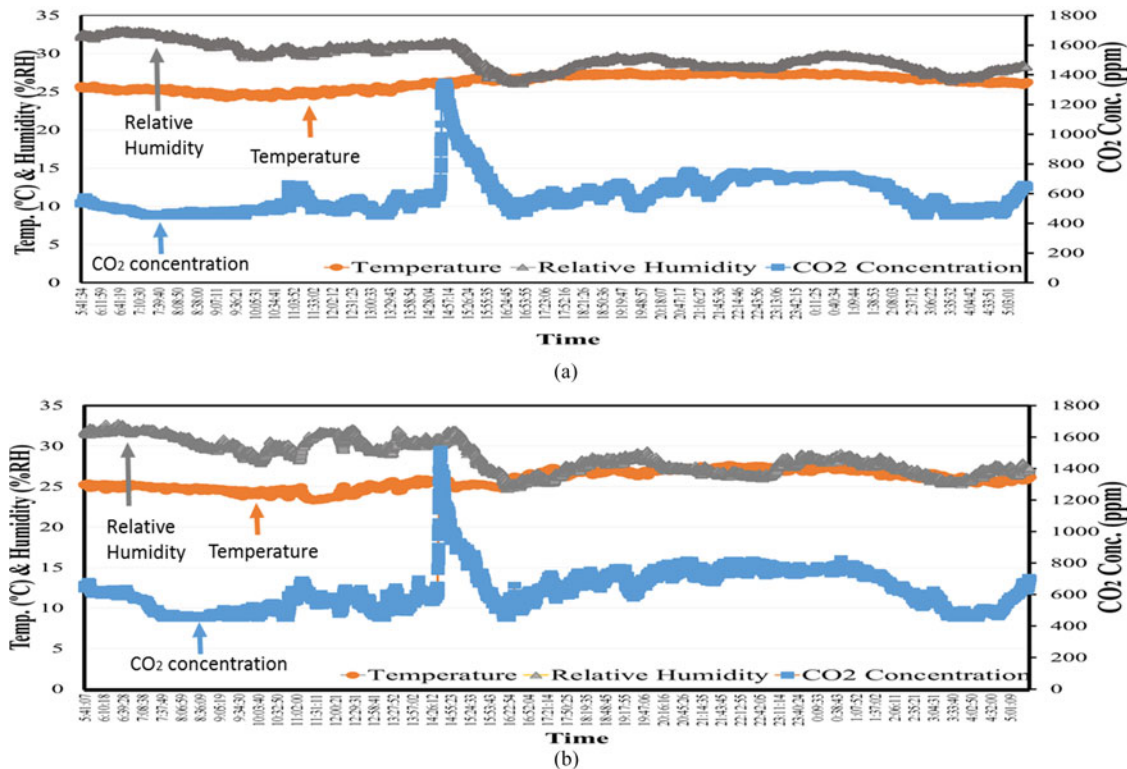
Fig. 6. Environment data from two sensor modules at two different locations in an office over 24 hours. (a) Sequential data from sensor module #1. (b) Sequential data from sensor module #2.

values in the HSV color representation. The lowest hue level is red, followed by yellow, green, blue, and pink in the ascending order. Nonetheless, the two sensor modules implemented the same color representations, and different reference values for each color were set for the two sets of received data. Differences in the transmission distance, angle of light radiation, environment light intensity, and background color of sensor module locations caused the differences in the hue values of the demodulated colors. In spite of these differences, the two sets of data can still be classified into the corresponding colors correctly as shown in the Fig. 5. There are a few points indicated by the red circle which fall between two color levels, slightly higher or slightly lower than any color level are error data. These error data only occur once during the color transition of the LED. These error data are collected owing to the high ratio between the exposure time of the camera and the LED transition time. The LED transition time is extremely short compared to the exposure time of the camera. During the exposure period of a single frame, the CMOS sensor continuously collects light information from the LED. If the LED changes from one color to another color during the exposure period of the camera, part of the previous light information is collected and the other part will be the current light information. Therefore, the information collected by the CMOS sensor is the combination of two colors. Random data are collected and they depend on the ratio of the two color information collected. As the frame rate is four times faster than the data rate, four frames are captured during a single bit period. Using the redundant data, a de-bouncing algorithm is used to cancel out all single point which are not continuously detected to minimize the error rate in the system.

For the validation of our proposed indoor environment monitoring system, we monitored the environment data received from two sensor modules at two different locations in an office for 24 hours as shown in Fig. 6. In the tests, as no one was present in the office during Saturday morning between 5 am and 2 pm and Sunday night between 2 am and 5 am, the CO_2 concentrations in
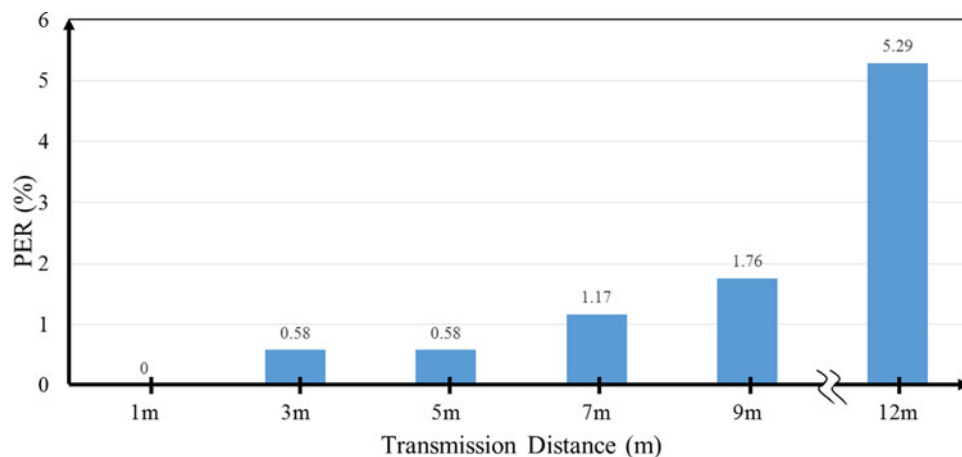
Fig. 7. Packet errors at different distances.

the two areas were maintained at a healthy level even though the windows and doors were closed. During Saturday afternoon, five persons came to the office. The CO_2 concentration increased rapidly to an unhealthy level. The data from the sensor module #2 showed a higher value, 1600 ppm, as more people were gathered in this area compared to the other area. At 3 pm, the CO_2 concentrations of both locations decreased gradually as the windows were opened. The CO_2 concentration was maintained at an acceptable level of 800 ppm from 4 pm to 2 am. The temperature within the office was maintained at 26 ± 1 °C at sensor module #1s location, and at 25 ± 1 °C at sensor module #2s location. The humidity at both locations was high during the period between 5 am and 3 pm due to rain, and dropped slowly to below 30% RH after the rain stopped.

The transmission error rate in the proposed mobile VLC system was measured by the transmission of a set of dummy data at different transmission distances from 1 m to 12 m, as shown in Fig. 7. The packet error rate (PER) calculation includes error data and data loss. Lower packet error rates were observed for transmission distances less than 7 m. This is because a much clearer and sufficiently large data signal can be captured within 7 m. The LED light signal becomes smaller as the transmission distance increases; this causes a weak and small LED signal to be captured. The increasing possibility of information loss causes incorrect data to be demodulated or data to be lost. Hence, the PER increases at transmission distances beyond 7 m, and the average PER is 5.29% at the maximum distance of transmission, that is, 12 m. Moreover, using proposed FSK scheme we able to achive a higher data rate (four times) with a lower error rate in the distance less than 10 m compare to the results of our previous OOK method reported in [24]. Yet, we can extend the transmission distance with lower data loss by using a high power LED lighting device with a large radiation angle or external camera zoom lenses, which able to reflect the light power over long distances. The transmission distance may also be increased by using a high resolution IS, which can provide more pixels within a single image.

6. Conclusion

Majority of the people spend more than 90% of their time staying in indoor environments. These indoor environments can change without the humans being aware of these changes, which may cause various health problems. Therefore, long term real-time hazardless environment monitoring systems are essential to maintain a healthy environment. A long range EMI-free mobile camera sensor-based environment monitoring system with VLC technology was developed and applied for the low complexity multi-location indoor environment monitoring. Multiple indoor environment data were monitored wirelessly, continuously, and simultaneously using a single mobile device. A reliable multiple input VLC transmission with low PER was achieved for transmission distances in

the range from 1 m to 12 m. The developed system can be applied to monitor indoor environments in areas inhabited by people with weak immune systems such as patients, elderly people, babies, or children, to prevent long term exposure to RF waves. It also supports the possibility of implementing wireless environment monitoring systems in RF-sensitive areas such as hospitals with high precision instruments, residential-care facilities for the elderly, aircrafts, spaceships, etc.

References

[1] BBC News, "Intelligent Machines: The jobs robots will steal first," Sep. 14, 2015. [Online]. Available: http://www.bbc.com/news/technology-33327659

[2] G. Zhou and Y. Chen, "The research of carbon dioxide gas monitoring platform based on the wireless sensor networks," in *Proc. 2nd Int. Conf. Artif. Intell., Manage. Sci. Electron. Commerce*, Aug. 8–10, 2011, pp. 7402–7405.

[3] R. C. Chen, H.-Y. Guo, M.-P. Lin, and H. S. Lin, "The carbon dioxide concentration detection using mobile phones combine bluetooth and QR code," in *Proc. IEEE 6th Int. Conf. Awareness Sci. Technol.*, Oct. 29–31, 2014, pp. 1–6.

[4] R. Li, X. Sha, and K. Lin, "Smart greenhouse: A real-time mobile intelligent monitoring system based on WSN," in *Proc. Int. Wireless Commun. Mobile Comput. Conf.*, Aug. 4–8, 2014, pp. 1152–1156.

[5] A. Ahlbom, A. Green, L. Kheifets, D. Savitz, and A. Swerdlow, "Epidemiology of health effects of radiofrequency exposure," *Environ. Health Perspect.*, vol. 112, no. 17, pp. 1741–1754, Dec. 2004, doi: 10.1289/ehp.7306.

[6] C. Ott *et al.*, "A humanoid two-arm system for dexterous manipulation," in *Proc. IEEE-RAS Int. Conf. Humanoid Robot.*, 2006, pp. 276–283.

[7] K. S. Tan, I. Hinberg, and J. Wadhwani, "Electromagnetic interference in medical devices: Health Canada's past current perspectives and activities," in *Proc. IEEE Int. Symp. Electromagn. Compat.*, 2001, pp. 1283–1284.

[8] Y. K. Cheong, X. W . Ng, and W. Y. Chung, "Hazardless biomedical sensing data transmission using VLC," *IEEE Sens. J.*, vol. 13, no. 9, pp. 3347–3348, Sep. 2013, doi: 10.1109/JSEN.2013.2274329.

[9] Y. Y. Tan and W. Y. Chung, "Mobile health-monitoring system through visible light communication," *Bio-Med. Mater. Eng.*, vol. 24, no. 6, pp. 3529–3538, Sep. 2014.

[10] K. D. Langer *et al.*, "Exploring the potentials of optical-wireless communication using white LEDs," in *Proc. 13th Int. Conf. Transparent Opt. Netw.*, Stockholm, Sweden, 2011, pp. 1–5.

[11] A. Y. Ali, Z. Zhang, and B. Zong, "Pulse position and shape modulation for visible light communication system," in *Proc. Int. Conf. Electromagn. Adv. Appl.*, Palm Beach, FL, USA, 2014, pp. 546–549.

[12] S. Videv and H. Haas, "Practical space shift keying VLC system," in *Proc. IEEE Wireless Commun. Netw. Conf.*, Istanbul, Turkey, 2014, pp. 405–409.

[13] M. Noshad and M. Brandt-Pearce, "Hadamard-coded modulation for visible light communications," *IEEE Trans. Commun.*, vol. 64, no. 3, pp. 1167–1175, Mar. 2016.

[14] H. B. Cai, J. Zhang, Y. J. Zhu, J. K. Zhang, and X. Yang, "Optimal constellation design for Indoor MIMO visible light communications," *IEEE Commun. Lett.*, vol. 20, no. 2, pp. 264–267, Feb. 2016.

[15] P. Deng and M. Kavehrad, "Real-time software-defined single-carrier QAM MIMO visible light communication system," in *Proc. Integr. Commun. Navigat. Surveillance Conf.*, Herndon, VA, USA, 2016, pp. 5A3-1–5A3-11.

[16] K.-H. Lim, H. S. Lee, and W.-Y. Chung, "Multichannel visible light communication with wavelength division for medical data transmission," *J. Med. Imag. Health Informat.*, vol. 5, no. 8, pp. 1947–1951, Dec. 2015.

[17] M. Zhang, P. Zhao, and Y. Jia, "A 5.7 Km visible light communications experiment demonstration," in *Proc. 7th Int. Conf. Ubiquitous Future Netw.*, Sapporo, Japan, 2015, pp. 58–60.

[18] S. Arnon, "Image sensor based visible light communication," in *Visible Light Communication*. Cambridge, U.K.: Cambridge Univ. Press, 2015, pp. 223–250.

[19] N. Saha, M. S. Ifthekhar, N. T. Le, and M. J. Yeong, "Survey on optical camera communications: Challenges and opportunities," *IET Optoelectron.*, vol. 9, no. 5, pp. 172–183, Oct. 2015, doi: 10.1049/iet-opt.2014.0151.

[20] C. Danakis, M. Afgani, G. Povey, I. Underwood, and H. Haas, "Using a CMOS camera sensor for visible light communication," in *Proc. IEEE Globecom Workshops*, Dec. 3–7, 2012, pp. 1244–1248, doi: 10.1109/GLOCOMW.2012.6477759.

[21] T. Nguyen, C. H. Hong, N. T. Le, and M. J. Yeong, "High-speed asynchronous optical camera communication using LED and rolling shutter camera," in *Proc. 7th Int. Conf. Ubiquitous Future Netw.*, Jul. 7–10, 2015, pp. 214–219.

[22] R. Boubezari, H. L. Minh, Z. Ghassemlooy, A. Bouridane, and A. TPham, "Data detection for smartphone visible light communications," in *Proc. 9th Int. Symp. Commun. Syst., Netw. Digit. Signal Process.*, Jul. 23–25, 2014, pp. 1034–1038.

[23] T. Nguyen, N. T. Le, and M. J. Yeong, "Practical design of screen-to-camera based optical camera communication," in *Proc. Int. Conf. Inf. Netw.*, Jan. 12–14, 2015, pp. 369–374.

[24] Z. Ong and W. Y. Chung, "Long range VLC temperature monitoring system using CMOS of mobile device camera," *IEEE Sens. J.*, vol. 16, no. 6, pp. 1508–1509, Mar. 15, 2016.

[25] V. P. Rachim, Y. Jiang, H. S. Lee, and W. Y. Chung, "Demonstration of long-distance hazard-free wearable EEG monitoring system using mobile phone visible light communication," *Opt. Exp.*, vol. 25, pp. 713–719, 2017.

[26] P. Luo *et al.*, "Experimental demonstration of RGB LED-based optical camera communications," *IEEE Photon. J.*, vol. 7, no. 5, pp. 1–12, Oct. 2015.

[27] V. Bradshaw, "Human comfort and health requirements," in *The Building Environment: Active and Passive Control Systems*, 3rd ed. Hoboken, NJ, USA: Wiley, May 2006, pp. 4–37.

[28] *Thermal Environmental Conditions for Human Occupancy*, Standard 55, ASHRAE Inc., Atlanta, GA, USA, 2013.

[29] *Ventilation for Acceptable Indoor Air Quality*, Standard 62.1, ASHRAE Inc., Atlanta, GA, USA, 2013.